

RADIATION FROM TAPERED DIELECTRIC ROD AERIALS

BY ANAND KUMAR AND MRS. RAJESWARI CHATTERJEE

(Department of Electrical Communication Engineering, Indian Institute of Science, Bangalore 12, India)

[Received: March 4, 1968]

ABSTRACT

Approximate expressions for the radiated field of a tapered dielectric rod aerial have been derived employing Schelkunoff's equivalence principle. Using these expressions H-plane radiation patterns for some of the aerials have been computed and these are compared with the experimentally observed patterns. Both the number and the relative amplitudes of minor lobes are found to decrease with increasing taper angle of the aerial.

1. INTRODUCTION

The possibility of using a suitably dimensioned and properly excited dielectric rod as an efficient directive aerial was examined experimentally by Mallach¹ some time before 1938. Following him, many authors²⁻¹⁸ have studied dielectric rod aerials both experimentally and theoretically. Various theoretical approaches have been made to derive radiation patterns of a dielectric rod aerial but the one based on Schelkunoff's equivalence principle¹⁹ appears to be the most successful of these.

Some experimental work has been done by Mueller and Tyrrell³ and Halliday and Kiely⁴ on a tapered dielectric rod aerial. They have reported that tapering the rod matches it to free-space, minimizes reflections at the free-end and gives smaller side lobes. As this aerial promises better characteristics and offers another controllable design parameter namely, its taper angle, a detailed study of the tapered dielectric rod aerial has been taken up at 3 cm. wavelength.

2. THEORETICAL

The most rigorous approach to the problem of determining the radiation field of any aerial would be the solution of Maxwell's electromagnetic field equations to satisfy the proper boundary conditions. For the tapered dielectric rod aerial, shown in Fig. 1, it has not been possible to apply this method because of the difficulty of obtaining a solution for the field to satisfy the boundary conditions on the surface of the rod, at the feed-end of the

aerial as well as at infinity²⁰. Hence the method employed in the present work for the calculation of the radiation field is approximate and is as follows²¹:

- (i) An approximate estimate of the source field, defined as the field existing on the surface of the tapered dielectric rod aerial, has been made.
- (ii) Using this approximate value of the field on the surface of the aerial, its radiation field has been calculated employing Schelkunoff's equivalence principle.

2.1. SOURCE FIELD

An attempt to determine the source field has been made²⁰ by solving Maxwell's electromagnetic field equations subject to the boundary conditions on the surface of the aerial. It is found that pure *E*-modes or *H*-modes do not exist on a semi-infinite conically tapered circular dielectric rod. It is also found that a linear combination of an *E*-mode and an *H*-mode forming an *HE*-mode is not possible.

As the above method fails to give the source field of the aerial, an approximate estimate of the source field is obtained by extending the analysis of a circular cylindrical infinitely long dielectric rod, whose propagation characteristics have been studied in detail by many workers²². The extension

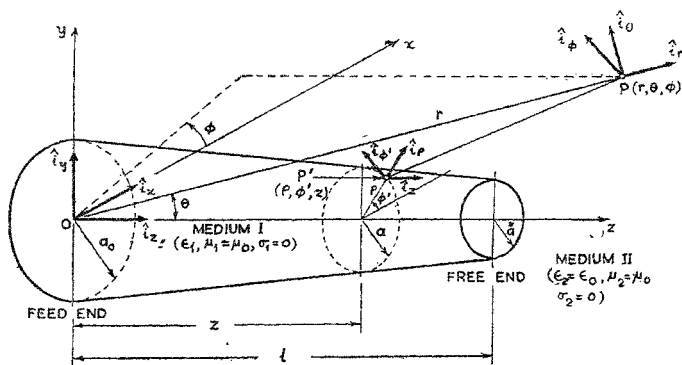


FIG. 1

Tapered dielectric rod aerial and coordinate systems

consists of assuming that the field at a point on the tapered dielectric rod aerial is the field that would exist on an untapered circular cylindrical infinitely long dielectric rod having its diameter equal to the diameter of the tapered aerial at that point. This means that the parameters of propagation, like the phase constant, which depend on the diameter of the rod are no longer constants but depend on the distance along the axis of the aerial.

The source field ($\underline{E}^i, \underline{H}^i$), therefore, is taken to be (using cylindrical coordinates (ρ, ϕ', z) - the z -axis being coincident with the axis of the aerial)^{23, 24}.

$$\left. \begin{aligned} E_{\rho}^i &= \eta_1^m H_{\phi'}^m + \delta \eta_1^e E_{\phi'}^e \\ E_{\phi'}^i &= -\eta_1^m H_{\rho}^m - \delta \eta_1^e E_{\rho}^e \\ E_z^i &= E_z^e \\ H_{\rho}^i &= H_{\rho}^m + \delta \cdot E_{\phi'}^e \\ H_{\phi'}^i &= H_{\phi'}^m + \delta \cdot E_{\rho}^e \\ H_z^i &= H_z^m \end{aligned} \right\} \quad [1]$$

where

$$\left. \begin{aligned} H_{\rho}^m &= A_1' (k_1 / \eta_1^m) J_1'(k_1 \rho) \cos \phi' \cdot \exp(-j \beta_1 z) \\ E_{\rho}^e &= A_1' (1 / \rho) J_1(k_1 \rho) \cos \phi' \cdot \exp(-j \beta_1 z) \\ H_{\phi'}^m &= -A_1' (1 / \eta_1^m \rho) J_1(k_1 \rho) \sin \phi' \cdot \exp(-j \beta_1 z) \\ E_{\phi'}^e &= -A_1' k_1 J_1'(k_1 \rho) \sin \phi' \cdot \exp(-j \beta_1 z) \\ H_z^m &= A_1' j (k_1^2 / \omega \mu_0) J_1(k_1 \rho) \cdot \cos \phi' \cdot \exp(-j \beta_1 z) \\ E_z^e &= -A_1' j (k_1^2 / \omega \epsilon_1) \delta J_1(k_1 \rho) \cdot \sin \phi' \cdot \exp(-j \beta_1 z) \end{aligned} \right\} \quad [2]$$

and

$$\left. \begin{aligned} \eta_1^e &= \beta_1 / \omega \epsilon_1 \\ \eta_1^m &= \omega \mu_0 / \beta_1 \\ \beta_1 &= \sqrt{\omega^2 \mu_0 \epsilon_1 - k_1^2} \end{aligned} \right\} \quad [3]$$

k_1 , β_1 , η_1^m , η_1^e and δ are functions of z . Variations of k_1 and δ with a/λ_0 are given in Fig. 2.²¹

2.2 RADIATION FIELD

Schelkunoff's equivalence principle¹⁹ has been made use of to calculate the radiation field from a knowledge of the aperture field²⁵. This principle, briefly stated is: In order to compute the electromagnetic field inside a source-free region bounded by a closed surface S , the given source distribution outside S can be replaced by a distribution of electric and magnetic currents over the surface S . The linear current densities of this equivalent source distribution are given by

$$\left. \begin{aligned} \underline{K}_i^e &= \hat{n} \times \underline{H}^i \\ \underline{K}_i^m &= -\hat{n} \times \underline{E}^i \end{aligned} \right\} \quad [4]$$

where, $(\underline{E}^i, \underline{H}^i)$ is the field distribution over the closed surface S and \hat{n} is a unit normal (inward) vector on S .

The radiation field at a point (γ, θ, ϕ) due to a current distribution is given by²⁶

$$E_\theta = \eta_0 H_\phi = -(j/2\lambda_0) \exp(-j\beta_0 r/r) [\eta_0 L_\theta^m + L_\theta^e] \quad [5]$$

$$E_\phi = -\eta_0 H_\theta = -(j/2\lambda_0) \exp(-j\beta_0 r/r) [\eta_0 L_\phi^m - L_\phi^e] \quad [6]$$

Where, the electric radiation vector \underline{L}^e and the magnetic radiation vector \underline{L}^m of the current distribution are given by

$$\underline{L}^e = \int_{\text{space}} \exp(j\beta_0(r - \overline{PP}')) \underline{dp}^e \quad [7]$$

$$\underline{L}^m = \int_{\text{space}} \exp(j\beta_0(r - \overline{PP}')) \underline{dp}^m \quad [8]$$

where,

$$\begin{aligned} \overline{PP}' &= \text{distance of the point } P(r, \theta, \phi) \text{ from the source point } P'(\rho, \theta', z) \\ r - \overline{PP}' &= z \cos \theta + \rho \sin \theta \cdot \cos(\phi - \phi') \end{aligned} \quad [9]$$

\underline{dp}^e and \underline{dp}^m are the moments of electric and magnetic current elements situated at the source point $P'(\rho, \phi', z)$ and are given by

$$\begin{aligned} \underline{dp}^e &= \underline{K}_i^e ds = (\hat{n} \times \underline{H}^i) ds \\ \underline{dp}^m &= \underline{K}_i^m ds = -(\hat{n} \times \underline{E}^i) ds \end{aligned} \quad [10]$$

where ds is an element of area located at the source point P' .

Substituting equations [9] and [10] in the equations [7] and [8], we get

$$\underline{L}^e = - \int_S \langle \exp j \beta_0 [z \cos \theta + \rho \sin \theta \cdot \cos(\phi - \phi')] \rangle (\hat{n} \times \underline{E}') \cdot ds \quad [11]$$

$$\text{and } \underline{L}^m = \int_S \langle \exp j \beta_0 [z \cos \theta + \rho \sin \theta \cos(\phi - \phi')] \rangle (\hat{n} \times \underline{H}') \cdot ds \quad [12]$$

In the case of the tapered dielectric rod aerial, let S consist of three parts— S_1 , S_2 and S_3 —as shown in Fig. 3, where,

S_1 = the conical surface of the tapered dielectric rod aerial

S_2 = the circular plane sources at the free-end of the aerial

and S_3 = the surface which together with S_1 and S_2 forms a closed surface outside which all the sources lie. S_3 consists of two portions—one coincides with the surface of the metal waveguide used for the excitation of the aerial and the other is a sphere of infinitely large radius about the origin.

The field is assumed to vanish at infinity so that the field everywhere on the spherical portion of S_3 is vanishingly small. The tangential components of the field over the portion of the surface S_3 enclosing the metal waveguide are assumed to be zero. This is a good approximation for the electric vector because the waveguide wall is a good conductor. However, the tangential magnetic field may exist. But this is neglected for the sake of simplicity. Under these assumptions the integrations in equations [11] and [12] are required to be carried out over S_1 and S_2 only. It is further assumed that the taper angle θ_0 of the aerial is so small that on the surface S_1 ,

$$\hat{n} \sim \hat{i}_\rho \quad \text{and} \quad ds \sim a \, dz \cdot d\phi' \quad [13]$$

S_1 is defined by

$$\rho = a(z) = a_0 - z \tan \theta_0, \quad 0 \leq \phi' \leq 2\pi, \quad 0 \leq z \leq 1 \quad [14]$$

and S_2 is defined by

$$0 \leq \rho \leq a^* = a_0 - 1 \tan \theta_0, \quad 0 \leq \phi' \leq 2\pi, \quad z = 1 \quad [15]$$

On S_2 ,

$$\hat{n} = \hat{i}_z, \quad ds = \rho \, d\rho \cdot d\phi' \quad [16]$$

In view of equations [13] to [16], equations [11] and [12] yield,

$$\begin{aligned} L_z^i = & - \int_0^1 \int_0^{2\pi} \{ \exp j \beta_0 [z \cos \theta + a \sin \theta \cos (\phi - \phi')] \} E_z^i \sin \phi' a d\phi' \cdot dz \\ & + \int_0^a \int_0^{2\pi} \{ \exp j \beta_0 [1 \cos \theta + \rho \sin \theta \cos (\phi - \phi')] \} (E_\phi^i \sin \phi' \\ & + E_\phi^i \cos \phi') \rho d\phi' d\rho \end{aligned} \quad [17]$$

$$\begin{aligned} L_z^e = & \int_0^1 \int_0^{2\pi} \{ \exp j \beta_0 [z \cos \theta + a \sin \theta \cos (\phi - \phi')] \} E_z^i \cos \phi' \cdot a d\phi' \cdot dz \\ & + \int_0^a \int_0^{2\pi} \{ \exp j \beta_0 [1 \cos \theta + \rho \sin \theta \cos (\phi - \phi')] \} (E_\phi^i \sin \phi' \\ & - E_\phi^i \cos \phi') \rho d\phi' d\rho \end{aligned} \quad [18]$$

$$L_z^i = - \int_0^1 \int_0^{2\pi} \{ \exp j \beta_0 [z \cos \theta + a \sin \theta \cos (\phi - \phi')] \} E_\phi^i a d\phi' dz \quad [19]$$

$$\begin{aligned} L_x^e = & \int_0^1 \int_0^{2\pi} \{ \exp j \beta_0 [z \cos \theta + a \sin \theta \cos (\phi - \phi')] \} H_z^i \sin \phi' \cdot a d\phi' \cdot dz \\ & - \int_0^a \int_0^{2\pi} \{ \exp j \beta_0 [1 \cos \theta + \rho \sin \theta \cos (\phi - \phi')] \} (H_\phi^i \sin \phi' \\ & + H_\phi^i \cos \phi') \rho d\phi' \cdot d\rho \end{aligned} \quad [20]$$

$$\begin{aligned} L_x^e = & \int_0^1 \int_0^{2\pi} \{ \exp j \beta_0 [z \cos \theta + a \sin \theta \cos (\phi - \phi')] \} H_z^i \cos \phi' \cdot a d\phi' \cdot dz \\ & + \int_0^a \int_0^{2\pi} \{ \exp j \beta_0 [1 \cos \theta + \rho \sin \theta \cos (\phi - \phi')] \} (H_\phi^i \cos \phi' \\ & - H_\phi^i \sin \phi') \rho d\phi' d\rho \end{aligned} \quad [21]$$

$$L_z^e = \int_0^1 \int_0^{2\pi} \{ \exp j \beta_0 [z \cos \theta + a \sin \theta \cos (\phi - \phi')] \} H_\phi^i \cdot a d\phi' \cdot dz \quad [22]$$

Substituting in equations [17] to [22] the values of (E^i, H^i) from equations [1] and [2], we obtain

$$\begin{aligned}
L_x^* &= \frac{j A_1'}{\omega \epsilon_1} \int_0^1 \int_0^{2\pi} \{\exp j [\beta z + x \cos (\phi - \phi')]\} \delta k_1 r J_1(r) \sin^2 \phi' d\phi' dz \\
&- A_1' \{\exp j \beta l \int_0^{\frac{\pi}{2}} \int_0^{2\pi} \{\exp j x' \cos (\phi - \phi') [J_1(R) \\
&\quad + \delta \overset{*}{\eta}_1^* R J_1'(R)]\} \sin^2 \phi' d\phi' \cdot d\rho \\
&- A_1' \{\exp j \beta l \int_0^{\frac{\pi}{2}} \int_0^{2\pi} \{\exp j x' \cos (\phi - \phi') [R J_1'(R) \\
&\quad + \delta \overset{*}{\eta}_1^* J_1(R)]\} \cos^2 \phi' d\phi' d\rho \quad [23]
\end{aligned}$$

$$\begin{aligned}
L_y^* &= -\frac{j A_1'}{\omega \epsilon_1} \int_0^1 \int_0^{2\pi} \{\exp j [\beta z + x \cos (\phi - \phi')]\} \delta k_1 r J_1(r) \sin \phi' \cos \phi' \cdot d\phi' dz \\
&+ A_1' \{\exp j \beta l (1 - \overset{*}{\delta} \overset{*}{\eta}_1) \int_0^{\frac{\pi}{2}} \int_0^{2\pi} \{\exp j x' \cos (\phi - \phi') [J_1(R) \\
&\quad - R J_1'(R)]\} \sin \phi' \cos \phi' d\phi' \cdot d\rho \quad [24]
\end{aligned}$$

$$L_z^* = A_1' \int_0^1 \int_0^{2\pi} \{\exp j [\beta z + x \cos (\phi - \phi')]\} [r J_1'(r) + \delta \eta_1^* J_1(r) \cos \phi' d\phi' \cdot dz \quad [25]$$

$$\begin{aligned}
L_x^m &= \frac{j A_1'}{\omega \mu_0} \int_0^1 \int_0^{2\pi} \{\exp j [\beta z + x \cos (\phi - \phi')]\} k_1 r J_1(r) \cos^2 \phi' d\phi' \cdot dz \\
&- A_1' \{\exp j \beta l \left(\frac{1}{\overset{*}{\eta}_1^m} - \overset{*}{\delta} \right) \int_0^{\frac{\pi}{2}} \int_0^{2\pi} \{\exp j x' \cos (\phi - \phi')\} [R J_1'(R) \\
&\quad - J_1(R)] \cos \phi' \sin \phi' d\phi' d\rho \quad [26]
\end{aligned}$$

$$\begin{aligned}
L_y^m &= -\frac{j A_1'}{\omega \mu_0} \int_0^1 \int_0^{2\pi} \{\exp j [\beta z + x \cos (\phi - \phi')]\} k_1 r J_1(r) \cos^2 \phi' d\phi' dz \\
&+ A_1' \{\exp j \beta l \int_0^{\frac{\pi}{2}} \int_0^{2\pi} \{\exp j x' \cos (\phi - \phi')\} \left[\frac{R}{\overset{*}{\eta}_1^m} J_1'(R) + \overset{*}{\delta} J_1(R) \right] \times \\
&\quad \cos^2 \phi' d\phi' \cdot d\rho \\
&+ A_1' \{\exp j \beta l \int_0^{\frac{\pi}{2}} \int_0^{2\pi} \{\exp j x' \cos (\phi - \phi')\} \left[\frac{1}{\overset{*}{\eta}_1^m} J_1(R) + \overset{*}{\delta} R J_1'(R) \right] \times \\
&\quad \sin^2 \phi' d\phi' \cdot d\rho \quad [27]
\end{aligned}$$

$$L_z^m = -A_1' \int_0^1 \int_0^{2\pi} \{\exp j[\beta z + x \cos(\phi - \phi')]\} \left[\delta r \cdot J_1'(r) + \frac{1}{\eta_1^m} J_1(r) \right] \times \\ \sin \phi' \cdot d\phi' \cdot dz \quad [28]$$

Integrations over ϕ' in the integrals in equations [23] to [28] are easily carried out giving

$$L_x^e = A_1' \frac{2\pi j}{\omega \epsilon_1} \int_0^1 \{\exp j\beta z\} \delta k_1 r \cdot J_1(r) \left[\sin^2 \phi J_0(x) + \cos 2\phi \frac{J_1(x)}{x} \right] dz \\ - A_1' 2\pi \{\exp j\beta 1\} \int_0^{\frac{\pi}{2}} [(1 - \delta \eta_1^*) J_1(R) + \delta \eta_1^* R J_0(R)] \times \\ \left[\sin^2 \phi J_0(x') + \cos 2\phi \cdot \frac{J_1(x')}{x'} \right] d\rho \\ - A_1' 2\pi \{\exp j\beta 1\} \int_0^{\frac{\pi}{2}} [R J_0(R) - (1 - \delta \eta_1^*) J_1(R)] \times \\ \left[\cos^2 \phi J_0(x') - \cos 2\phi \frac{J_1(x')}{x'} \right] d\rho \quad [29]$$

$$L_y^e = -A_1' \frac{\pi j \sin 2\phi}{\omega \epsilon_1} \int_0^1 \{\exp j\beta z\} \delta k_1 r \cdot J_1(r) [J_0(x) - (2/x) J_1(x)] dz \\ + A_1' \{\exp j\beta 1\} \pi \sin 2\phi (1 - \delta \eta_1^*) \int_0^{\frac{\pi}{2}} [2 J_1(R) - R J_0(R)] J_0(x') \\ - (2/x') J_1(x') d\rho \quad [30]$$

$$L_z^e = A_1' 2\pi j \cos \phi \int_0^1 \{\exp j\beta z\} [r J_0(r) - (1 - \delta \eta_1^*) J_1(r)] J_1(x) dz \quad [31]$$

$$L_x^m = -A_1' \frac{\pi j \sin 2\phi}{\omega \mu_0} \int_0^1 \{\exp j\beta z\} k_1 r \cdot J_1(r) [(2/x) J_1(x) - J_0(x)] dz \\ - A_1' (1/\eta_1^m - \delta) \{\exp j\beta 1\} \pi \sin 2\phi \int_0^{\frac{\pi}{2}} [R J_0(R) - 2 J_1(R)] [(2/x') J_1(x') \\ - J_0(x')] d\rho \quad [32]$$

$$\begin{aligned}
L_z^m = & -j A_1' (2\pi' \omega \mu_0) \int_0^1 \{ \exp j \beta z \} k_1 r \cdot J_1(r) [\cos^2 \phi \cdot J_0(x') \\
& - \cos 2\phi \langle J_1(x)/x \rangle] dz \\
& + A_1' \{ \exp j \beta z \} 2\pi \int_0^{\frac{\pi}{2}} \left[(1/\eta_1^m) R J_1(R) - (\langle 1/\eta_1^m \rangle - \delta) J_1(R) \right] \times \\
& \quad [\cos^2 \phi \cdot J_0(x') - \cos 2\phi \langle J_1(x')/x' \rangle] d\rho \\
& + A_1' \{ \exp j \beta z \} 2\pi \int_0^{\frac{\pi}{2}} \left[\delta R J_0(R) + (\langle 1/\eta_1^m \rangle - \delta) J_1(R) \right] \\
& \quad [\sin^2 \phi J_0(x') + \cos 2\phi \langle J_1(x')/x' \rangle] d\rho \quad [33]
\end{aligned}$$

$$L_z^m = -j A_1' 2\pi \sin \phi \int_0^1 \exp(j\beta z) \left[\delta r J_0(r) + \left(\frac{1}{\eta_1^m} - \delta \right) J_1(r) \right] J_1(x) dz \quad [34]$$

Let

$$I_1 = \int_0^1 \exp(j\beta z) \delta k_1 r \cdot J_1(r) \{ \sin^2 \phi J_0(x) + \cos 2\phi [J_1(x)/x] \} dz \quad [35]$$

$$I_2 = \int_0^1 \exp(j\beta z) \delta k_1 r J_1(r) \left[2 \frac{J_1(x)}{x} - J_0(x) \right] dz \quad [36]$$

$$I_3 = \int_0^1 \exp(j\beta z) k_1 r J_1(r) \left[2 \frac{J_1(x)}{x} - J_0(x) \right] dz \quad [37]$$

$$I_4 = \int_0^1 \exp(j\beta z) k_1 r J_1(r) \left[\cos^2 \phi J_0(x) - \cos 2\phi \frac{J_1(x)}{x} \right] dz \quad [38]$$

$$I_5 = \int_0^1 \exp(j\beta z) [r J_0(r) - (1 - \delta \eta_1^m) J_1(r)] J_1(x) dz \quad [39]$$

$$I_6 = \int_0^1 \exp(j\beta z) \left[\delta r J_0(r) + \left(\frac{1}{\eta_1^m} - \delta \right) J_1(r) \right] J_1(x) dz \quad [40]$$

$$I_7 = \int_0^{\frac{\pi}{2}} R J_0(R) J_0(x') d\rho \quad [41]$$

$$I_8 = \int_0^{\frac{\pi}{2}} [2 J_1(R) - R J_0(R)] \left[2 \frac{J_1(x')}{x'} - J_0(x') \right] d\rho \quad [42]$$

In terms of the integrals I_1, I_2, \dots, I_8 , defined above, equations [29] to [34] become,

$$(1/A'_1) L_x^c = j(1/f\epsilon_1) I_1 - \pi (1 + \delta^* \eta_1^*) \exp(j\beta^* 1) I_7 - \pi (1 - \delta^* \eta_1^*) \times \\ \exp(j\beta^* 1) \cos 2\phi I_8 \quad [43]$$

$$(1/A'_1) L_y^c = j(1/2f\epsilon_1) \sin 2\phi I_2 - \pi (1 - \delta^* \eta_1^*) \exp(j\beta^* 1) \sin 2\phi I_8 \quad [44]$$

$$(1/A'_1) L_z^c = j 2\pi \cos \phi I_3 \quad [45]$$

$$(1/A'_1) L_x^m = -j(1/2f\mu_0) \sin 2\phi I_3 - \pi [(1/\eta_1^m) - \delta^*] \exp(j\beta^* 1) \sin 2\phi I_8 \quad [46]$$

$$(1/A'_1) L_y^m = -j(1/f\mu_0) I_4 + \pi [(1/\eta_1^m) + \delta^*] \exp(j\beta^* 1) I_7 + \pi \times \\ [(1/\eta_1^m) - \delta^*] \exp(j\beta^* 1) \cos 2\phi I_8 \quad [47]$$

$$(1/A'_1) L_z^m = -j 2\pi \sin \phi \cdot I_6 \quad [48]$$

From equations [43] to [48] $L_\theta^c, L_\theta^m, L_\phi^c$, and η_ϕ^m are obtained.

$$(1/A'_1) L_\theta^c L_\theta^c = j(1/f\epsilon_1) \cos \theta \cos \phi \cdot I_1 + j(1/2f\epsilon_1) \cos \theta \sin \phi \sin 2\phi \cdot I_2 \\ - j 2\pi \sin \theta \cos \phi \cdot I_5 - \pi (1 + \delta^* \eta_1^*) \exp(j\beta^* 1) \cos \theta \cos \phi \cdot I_7 \\ - \pi (1 - \delta^* \eta_1^*) \exp(j\beta^* 1) \cos \theta \cos \phi \cdot I_8 \quad [49]$$

$$(1/A'_1) L_\phi^c = -j(1/f\epsilon_1) \sin \phi \cdot I_1 + j(1/2f\epsilon_1) \sin 2\phi \cos \eta I_2 \\ + \pi (1 + \delta^* \eta_1^*) \exp(j\beta^* 1) \sin \phi I_7 - \pi (1 - \delta^* \eta_1^*) \exp(j\beta^* 1) \sin \phi \cdot I_8 \quad [50]$$

$$(1/A'_1) L_\theta^m = -j(1/2f\mu_0) \cos \theta \cos \phi \sin 2\phi I_3 - j(1/f\mu_0) \cos \theta \sin \phi I_4 \\ + j 2\pi \sin \theta \sin \phi \cdot I_6 + \pi [(1/\eta_1^m) + \delta^*] \exp(j\beta^* 1) \cos \theta \sin \phi \cdot I_7 \\ - \pi [(1/\eta_1^m) - \delta^*] \exp(j\beta^* 1) \cos \theta \sin \phi \cdot I_8 \quad [51]$$

$$(1/A'_1) L_\phi^m = j(1/2f\mu_0) \sin \phi \sin 2\phi \cdot I_3 - j(1/f\mu_0) \cos \phi \cdot I_4 \\ + \pi [(1/\eta_1^m) + \delta^*] \exp(j\beta^* 1) \cos \phi \cdot I_7 + \pi [(1/\eta_1^m) - \delta^*] \exp(j\beta^* 1) \cos \phi I_8 \quad [52]$$

Substitutions of equations [51] and [50] in the equation [5] and that of equations [52] and [49] in the equation [6] give

$$\begin{aligned}
 & (2 \lambda_0 r / A_1') j \exp (j \beta_0 r) E_\theta \\
 &= -j (1/f \epsilon_1) \sin \phi \cdot I_1 + j (1/2 f \epsilon_1) \cos \phi \cdot \sin 2 \phi \cdot I_2 \\
 & \quad -j (\lambda_0/2) \cos \theta \cos \phi \sin 2 \phi \cdot I_3 \\
 & \quad -j \lambda_0 \cos \theta \sin \phi \cdot I_4 + j 2 \pi \eta_0 \sin \theta \sin \phi \cdot I_6 \\
 & \quad -\pi \langle (1 + \delta \overset{*}{\eta}_1^*) + [(\overset{*}{\beta}_1/\beta_0) + \eta_0 \overset{*}{\delta}] \cos \theta \rangle \exp (j \overset{*}{\beta} l) \sin \phi \cdot I_7 \\
 & \quad -\pi \langle (1 - \delta \overset{*}{\eta}_1^*) + [(\overset{*}{\beta}_1/\beta_0) - \eta_0 \overset{*}{\delta}] \cos \theta \rangle \exp (j \overset{*}{\beta} l) \sin \phi \cdot I_8 \quad [53]
 \end{aligned}$$

and,

$$\begin{aligned}
 & (2 \lambda_0 r / A_1') j \exp (j \beta_0 r) E_\phi \\
 &= -j (1/f \epsilon_1) \cos \theta \cos \phi \cdot I_1 - j (1/2 f \epsilon_1) \cos \theta \sin \phi \sin \phi \cdot I_2 \\
 & \quad + j (\lambda_0/2) \sin \phi \sin 2 \phi \cdot I_3 - j \lambda_0 \cos \phi \cdot I_4 + j 2 \pi \sin \theta \cos \phi \cdot I_5 \\
 & \quad + \pi \langle (1 + \delta \overset{*}{\eta}_1^*) \cos \theta + [(\overset{*}{\beta}_1/\beta_0) + \eta_0 \overset{*}{\delta}] \exp (j \overset{*}{\beta} l) \cos \phi \cdot I_7 \\
 & \quad + \pi \langle (1 - \delta \overset{*}{\eta}_1^*) \cos \theta + [(\overset{*}{\beta}_1/\beta_0) - \eta_0 \overset{*}{\delta}] \exp (j \overset{*}{\beta} l) \cos \phi \cdot I_8 \quad [54]
 \end{aligned}$$

2.3. H-PLANE RADIATION PATTERN

Equations [53] and [54] give the radiation field of a tapered dielectric rod aerial at a distant point P (r, θ, ϕ). Therefore, the H-plane radiation pattern of the aerial is obtained by setting $\phi = 0^\circ$ and 180° . Hence, in the H-plane,

$$E_\theta = 0$$

$$\begin{aligned}
 & \text{and } (2 \lambda_0 r / A_1') j \{ \exp j \beta_0 r \} E_\phi \\
 &= \langle -j (1/f \epsilon_1) \cos \theta I_1 - j \lambda_0 I_4 + j 2 \pi \sin \theta \cdot I_5 \\
 & \quad + \pi [(1 + \delta \overset{*}{\eta}_1^*) \cos \theta + \{ (\overset{*}{\beta}_1/\beta_0) + \eta_0 \overset{*}{\delta} \}] \{ \exp j \overset{*}{\beta} l \cdot I_7 \\
 & \quad + \pi [(1 - \delta \overset{*}{\eta}_1^*) \cos \theta + \{ (\overset{*}{\beta}_1/\beta_0) - \eta_0 \overset{*}{\delta} \}] \{ \exp j \overset{*}{\beta} l \} \cdot I_8 \rangle [\cos \phi]_{\phi=0^\circ, 180^\circ} \\
 & \quad [55]
 \end{aligned}$$

$$\text{Now, in the H-plane, } E_y = E_\phi \cdot [\cos \phi]_{\phi=0^\circ, 180^\circ} \quad [56]$$

Substitution of the equation [56] in [55] gives

$$\begin{aligned} (2 \lambda_0 r / A_1') j \{ \exp j \beta_0 r \} E_y \\ = -j (1/f \epsilon_1) \cos \theta \cdot I_1 - j \lambda_0 I_4 + j 2\pi \sin \theta \cdot I_5 \\ + \pi [(1 + \delta \eta_1^*) \cos \theta + (\langle \beta_1 / \beta_0 \rangle + \eta_0 \delta^*)] \{ \exp j \beta^* 1 \cdot I_7 \\ + \pi [(1 - \delta \eta_1^*) \cos \theta + (\langle \beta_1 / \beta_0 \rangle - \eta_0 \delta^*)] \{ \exp j \beta^* 1 \cdot I_8 \end{aligned} \quad [57]$$

Values of the integrals appearing in the equation [57] are obtained from equations [35] to [42] by setting $\phi = 0^\circ$ or 180° in them. Thus,

$$I_1 = I_{1r} + j I_{1m} = \int_0^1 \{ \exp j \beta z \} \delta k_1 r \cdot J_1(r) \frac{J_1(x)}{x} dz \quad [58]$$

$$I_4 = I_{4r} + j I_{4m} = \int_0^1 \exp j \beta z \} k_1 r \cdot J_1(r) \left[J_0(x) - \frac{J_1(x)}{x} \right] dz \quad [59]$$

$$I_5 = I_{5r} + j I_{5m} = \int_0^1 \{ \exp j \beta z \} [r J_0(r) - (1 - \delta \eta_1^*) J_1(r)] J_1(x) dz \quad [60]$$

$$I_7 = \int_0^{\frac{\pi}{2}} R J_0(R) \cdot J_0(x') d\rho \quad [61]$$

$$I_8 = \int_0^{\frac{\pi}{2}} [2 J_1(R) - R J_0(R)] \left[2 \frac{J_1(x')}{x'} - J_0(x') \right] d\rho \quad [62]$$

Where the second subscripts 'r' and 'm' stand for the real and the imaginary parts respectively.

E_y can be written in the form

$$E_y = -A_1' \frac{\pi}{\lambda_0} \cdot \frac{\exp \{ -j \beta_0 r \}}{r} [E_{yr}^\dagger + j E_{ym}^\dagger] \quad [63]$$

where,

$$E_{yr}^\dagger = c_1 I_{1r} + c_4 I_{4r} + c_5 I_{5r} + c_{7r} I_7 + c_{8r} I_8 \quad [64]$$

$$\text{and } E_{ym}^\dagger = c_1 I_{1m} + c_4 I_{4m} + c_5 I_{5m} + c_{7m} I_7 + c_{8m} I_8 \quad [65]$$

with,

$$\begin{aligned}
 c_1 &= (60 \lambda_0 / \epsilon_{r1}) \cdot \cos \theta \\
 c_4 &= (\lambda_0 / 2\pi) \\
 c_5 &= -\sin \theta \\
 c_{7r} &= -\frac{1}{2} [(1 + \delta^* \eta_1^*) \cos \theta + (\{\beta_1^* / \beta_0^*\} + \eta_0^* \delta^*) \sin \beta^* l] \\
 c_{7m} &= \frac{1}{2} [(1 + \delta^* \eta_1^*) \cos \theta + (\{\beta_1^* / \beta_0^*\} + \eta_0^* \delta^*) \cos \beta^* l] \\
 c_{8r} &= -\frac{1}{2} [(1 - \delta^* \eta_1^*) \cos \theta + (\{\beta_1^* / \beta_0^*\} - \eta_0^* \delta^*) \sin \beta^* l] \\
 c_{8m} &= \frac{1}{2} [(1 - \delta^* \eta_1^*) \cos \theta + (\{\beta_1^* / \beta_0^*\} - \eta_0^* \delta^*) \cos \beta^* l]
 \end{aligned} \tag{66}$$

Therefore, the H-plane radiation pattern (field) of a tapered dielectric rod aerial is given by

$$|E_y| = a \text{ constant } \times \sqrt{E_{yr}^{\dagger 2} + E_{ym}^{\dagger 2}} \tag{67}$$

The integrals I_1 , I_4 , I_5 , I_7 and I_8 are evaluated numerically for every value of the angle θ , k_1 and δ are obtained from Fig. 2. β_1 is calculated from the equation [3] and hence η_1^* and η_1^m are calculated. Equations [66] give the values of the co-efficients, c 's, for every value of θ . In this way, E_{yr}^{\dagger} and E_{ym}^{\dagger} are calculated and hence the H-plane radiation pattern obtained.

3. EXPERIMENTAL

In order to test the equations derived in the preceding section, a large number of perspex rod aeriels of different lengths taper-angles and feed-end diameters have been constructed. Two sets of aeriels of feed-end diameters 2.5 cm and 1.9 cm and of lengths varying from $2\lambda_0$ to $6\lambda_0$ have been used. The aeriels fit snugly in metal waveguides of internal diameters equal to 2.5 cm and 1.9 cm respectively propagating the H_{11} -mode. The portion of the aerial (about $2\lambda_0$ in length) inside the metal waveguide is tapered to a point to avoid a sudden discontinuity.

Fig. 4 gives the schematic diagram of the experimental set up used to obtain the radiation pattern of the dielectric rod aeriels. The microwave power source consists of a type 723A/B reflex klystron operating at a frequency of 9375 MHz. ($\lambda_0 = 3.2$ cm). The reflector voltage of this klystron is modulated by a 1 k Hz square wave whose amplitude is so adjusted as to produce an 'on-off' modulation. The power travels in the H_{10} -mode in a rectangular metal waveguide type RG 51/U. A mode transformer is used to convert the H_{10} -mode in a rectangular metal waveguide into the H_{11} -mode

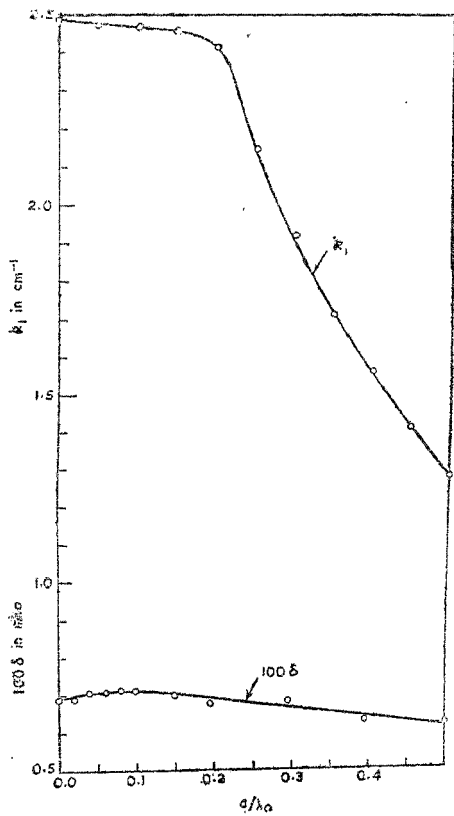


Fig. 2
Variation of k_1 and δ

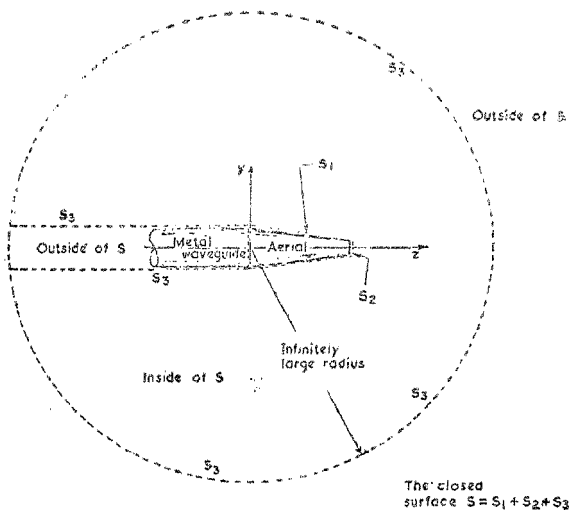
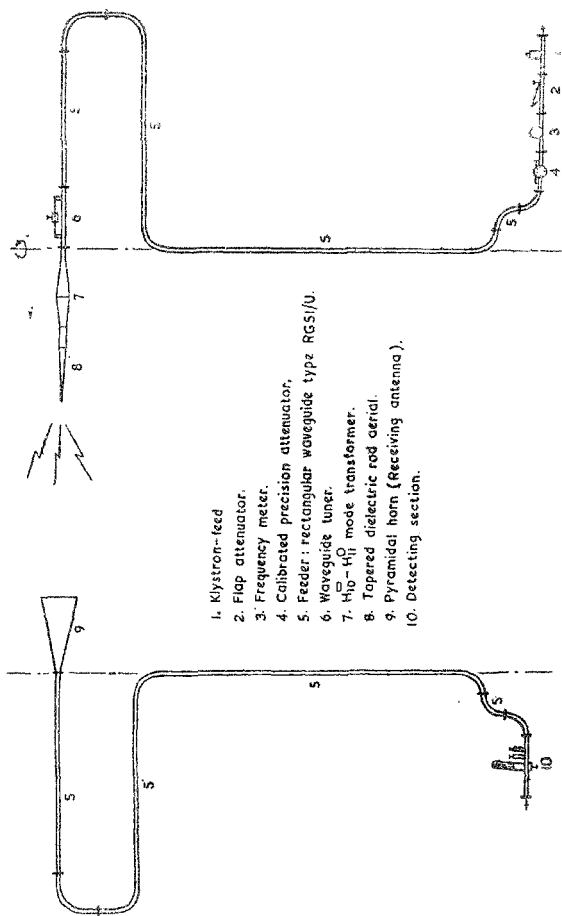


FIG. 3
Surface S

in the circular cylindrical metal waveguide which excites the aeriols. A portion of the power radiated by the aeriols is received by the receiving aerial—a 27.5 db. pyramidal horn. The received power travels a distance of about 4.5 metres down the feeder before it reaches the detecting action wherein it is detected by a 1N23B crystal diode. The output of the detector is amplified by an amplifier which is tuned to 1kHz . The output of the detector amplifier is found to vary linearly with the received power.

The aerial under test is rotated manually about a vertical axis and thus the aerial rotates in the horizontal plane (the H-plane of the system). H-plane radiation pattern is obtained by noting down the output of the detector amplifier for various angles of rotation of the aerial about the vertical axis. Fifty of the observed radiation patterns are reproduced here along with twenty four calculated patterns, which are shown in dotted lines. (ref. Fig. Nos. 5 to 14)



1. Klystron-feed
2. Flap attenuator.
3. Frequency meter.
4. Calibrated precision attenuator.
5. Feeder: rectangular waveguide type RGS/U.
6. Waveguide tuner.
7. $H_{10}-H_{11}$ mode transformer.
8. Tapered dielectric rod aerial.
9. Pyramidal horn (Receiving antenna).
10. Detecting section.

FIG. 4
Experimental set up for obtaining radiation pattern

4. CONCLUSIONS

All the observed patterns show spurious kinks and pips. The pattern wriggles more in the $\phi = 180^\circ$ region. This may be caused by stray reflections from surrounding objects, though these objects are quite far from the two aerials. (ref. Fig. 15).

The agreement between the observed and the calculated pattern is broadly satisfactory. In some cases, at the positions where distinct minor lobes are observed experimentally, only vestigial lobes appear in the calculated patterns. This smudging of the calculated pattern may be a result of the approximations made in the numerical computation of the pattern.

It is found that both the total number and the relative amplitudes of the minor lobes in the radiation pattern of a tapered dielectric rod aerial of a given axial length show a tendency to decrease with increasing taper angle.

5. ACKNOWLEDGMENTS

The authors are thankful to Dr. S. Dhawan, Director, Indian Institute of Science and to Prof. S. V. C. Aiyar, Head of the Electrical Communication Engineering Department for their encouragement and for the facilities provided. One of the authors (Anand Kumar) is grateful to the University Grants Commission, Government of India and to the National Institute of Sciences of India for the fellowships awarded to him during the course of these investigations. The authors are also thankful to Prof. S. K. Chatterjee for his helpful suggestions and for the discussions they have had with him. They are also thankful to the Hindustan Aeronautics Limited, Bangalore for providing computer facilities.

List of Symbols :

x, y, z = Cartesian coordinates

ρ, ϕ, z = Cylindrical coordinates

r, θ, ϕ = spherical coordinates

ϵ, μ, σ = permittivity, permeability and conductivity, respectively, of medium.

l, a_0, θ_0 = axial-length, feed-end radius and taper angle, respectively, of the aerial.

$a = a_0 - z \tan \theta_0$ = radius of the aerial at a distance z from the feed-end.

$\underline{E}, \underline{H}$ = electric and magnetic intensities, respectively, with appropriate suffixes.

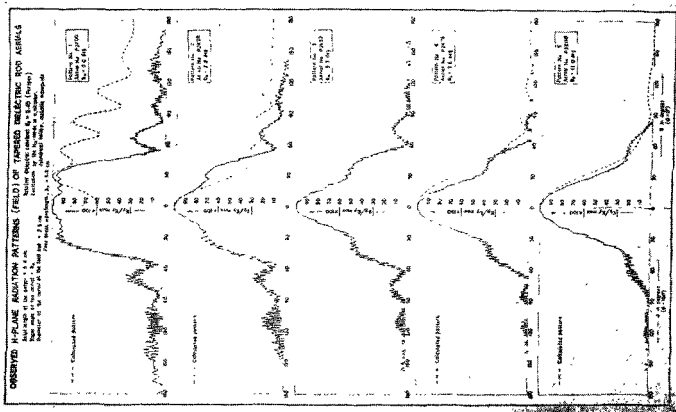
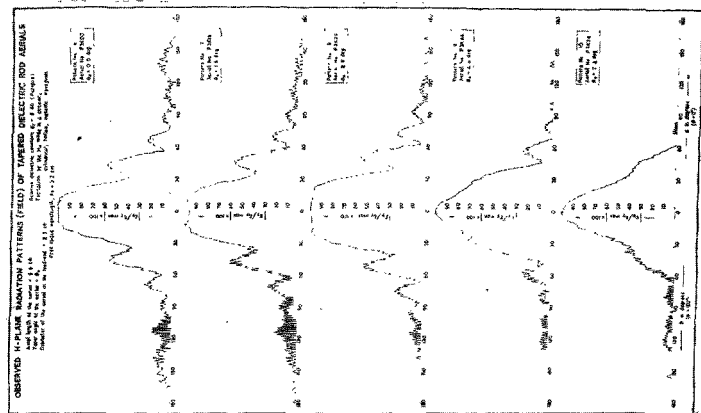


FIG. 5

FIG. 6

Radiation pattern

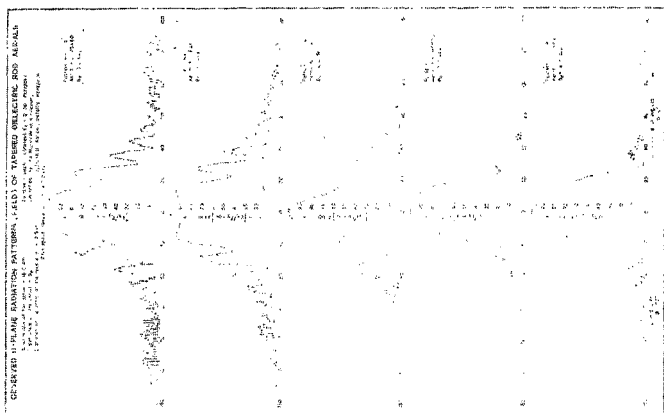


FIG. 8

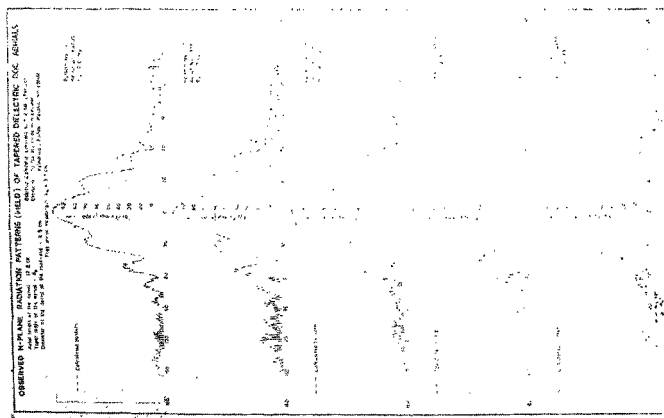


FIG. 7

Radiation pattern

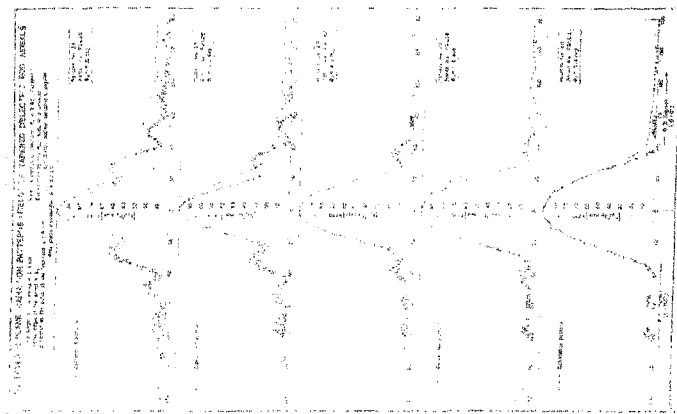


FIG. 10

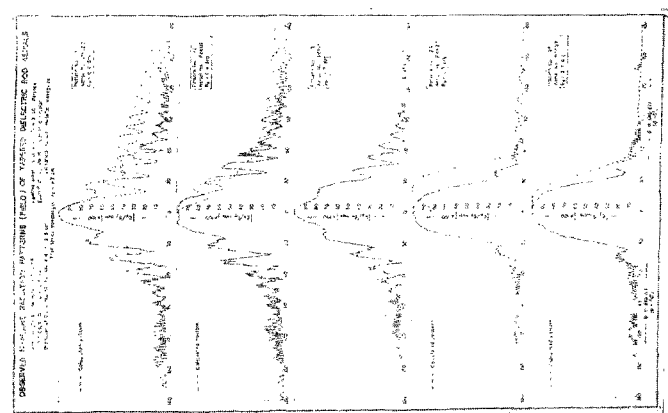


FIG. 9

Radiation pattern

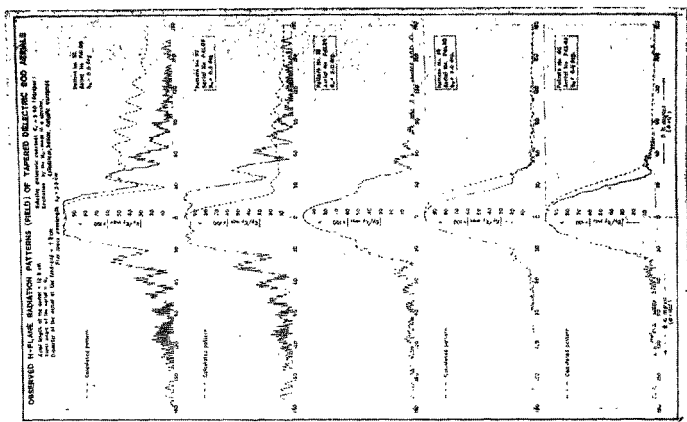


FIG. 12

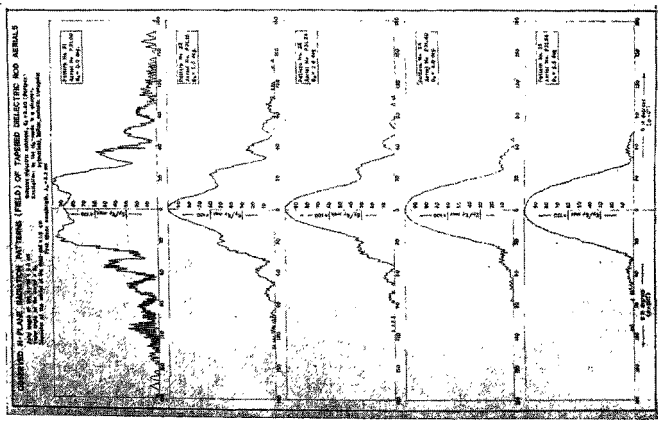


FIG. 11

Radiation pattern

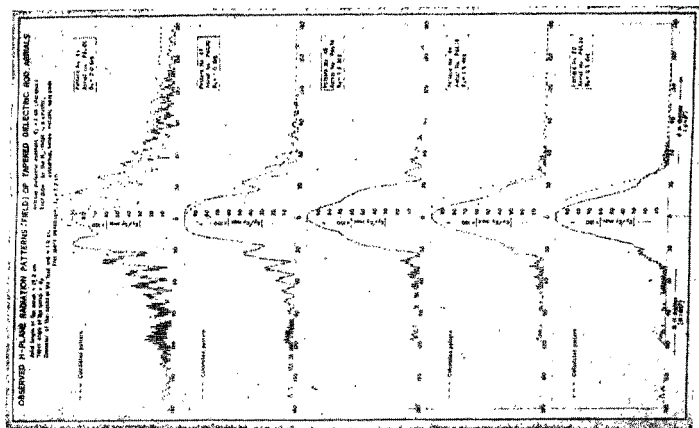


Fig. 13

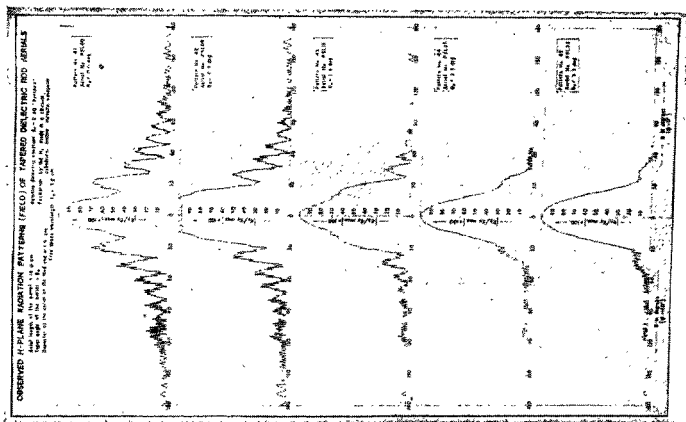


Fig. 14

Radiation pattern

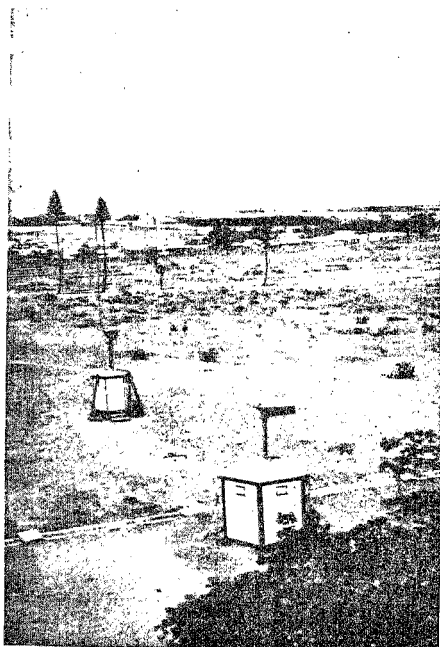


FIG. 15
Aerial view of Microwave Antenna Laboratory

A_1' = excitation constant for H -modes

δ = ratio of the excitation constants for E and H -modes

$k_1 = \sqrt{(\omega^2 \mu \epsilon_1 - \beta_1^2)}$

β_1 = phase coefficient of guided waves in the medium - I

η = wave impedance with appropriate suffixes

e = base of Napierian logarithm

$j = \sqrt{-1}$

$\omega = 2\pi f$

f = frequency

$J_\nu(z)$ = Bessel function of order ν and argument z

$J'_\nu(z) = (d/dz) J_\nu(z)$

$\beta_0 = (2\pi/\lambda_0)$

λ_0 = free space wavelength

$\beta = \beta_0 \cos \theta - \beta_1$

$x = \beta_0 a \sin \theta$

$\gamma = k_1 a$

$x' = \beta_0 \rho \sin \theta$

$R = R_1 \rho$

$\beta^*, \delta^*, \eta_1^*, \dots$ = values of $\beta, \delta, \eta_1^*, \dots$, respectively, at $z = l$

REFERENCES

1. Mallach, P. *Notes from unpublished German Documents Control Radio Bureau Library, London.*
2. Southworth, G. C. *U. S. Patent, 1941, 2, 206, 223.*
3. Mueller, G. E. and Tyrrell, W. A. *Bell Syst., Tech. Jour., 1947, 26, 837.*
4. Halliday, D. F. and Kiely, D. G. *J. Inst. elec. Engrs., 1947, 94, III A, 610.*
5. Chatterjee, R. and Chatterjee, S. K. *J. Indian Inst. Sci., 1957, 39, 134.*
6. ————— *J. Instrn. Telecommun. Engrs., 1957, 3, 280.*
7. Wilkes, G. *Proc. Inst. Radio Engrs. 1948, 36, 206.*
8. Watson, R. B. and Horton, C. W. *J. Appl. Phys., 1948, 19, 661.*
9. ————— *Ibid, 1948, 19, 836.*
10. Horton, C. W., Karal, F. C. and Mckinney, C. M. *Ibid, 1950, 21, 1. 79.*
11. Watson, R. B., *Ibid, 1951, 22, 154.*

- | | | | |
|-----|---|----|---|
| 12. | Chatterjee, R. and Chatterjee, S. K. | .. | <i>J. Indian Inst. Sci.</i> , 1956, 38, 93. |
| 13. | ————— | .. | <i>J. Inst. Engrs.</i> , 1958, 38, 1176. |
| 14. | Rao, B., Rama, Chatterjee, R. and Chatterjee, S. K. | .. | <i>J. Indian Inst. Sci.</i> , 1957, 39, 143. |
| 15. | Ramanujam, H. R. and Chatterjee, R. | .. | <i>Ibid</i> , 1962, 44, 164. |
| 16. | Brown, J. and Spector, J. O. | .. | <i>Proc. Instn. elect. Engrs.</i> , 1957, 104B, 27. |
| 17. | Makimoto, T., Sueta T. and Nishimura, S. | .. | <i>Mem Inst. Scient. Ind. Res., Osaka Univer.</i> 1961. |
| 18. | Ramanujam, H. R. and Chatterjee, R. | .. | <i>J. Indian Inst. Sci.</i> , 1962, 44, 203. |
| 19. | Schelkunoff, S. A. | .. | <i>Bell. Syst. tech. J.</i> , 1936, 15, 92. |
| 20. | Andnd Kumar, and Chatterjee, R. | .. | <i>J. Instn. Telecommun. Engrs.</i> , 1962, 8, 171. |
| 21. | ————— | .. | <i>Ph. D. Thesis, Indan Inst. Sci.</i> , 1965. |
| 22. | Subramaniam, V. | .. | <i>Ibid</i> , 1964. |
| 23. | Kiely, D. G. | .. | Mathuen's Monographs on Physical Subjects, Mathuen and Co., Ltd., 1958, 21, |
| 24. | Subrahmaniam, V. | .. | <i>J. Indian Inst. Sci.</i> , 1962, 44, 148. |
| 25. | Schelkunoff, S. A. | .. | <i>Phys. Rev.</i> , 1939, 56, 308. |
| 26. | ————— | .. | <i>Proc. Inst. Radio Engrs.</i> , 1939, 27, 660. |